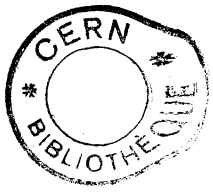

CERN/EP/3627R/AP/ed
15 September 1987

THE CERN Ω — WA76 EXPERIMENT: LIGHT MESON SPECTROSCOPY IN THE CENTRAL REGION

Antimo Palano

CERN, European Organization for Nuclear Research, Geneva, Switzerland

and

Dipartimento di Fisica, University of Bari, Italy

Geneva, 25 September 1987

Abstract: The main results coming from the Ω WA76 experiment of the exclusive study of mesons produced centrally in a search for glueballs and exotic states are reviewed.

Talk given at the International School of Physics with Low Energy Antiprotons

2nd Course: Spectroscopy of Light and Heavy Quarks

23 – 31 May 1987, Erice, Italy

1. Physics motivations

One of the basic expectations of the present theory of the strong interactions, QCD, is the existence of hadrons composed of gluons rather than quarks. The search for these new states, the glueballs, has been carried out in several experiments and has led to the discovery of a few candidates. However, the still undefined situation in the field of light meson spectroscopy makes it difficult to establish them as glueball states since the possibility that they are 4 − quark states or radial excitations cannot be ruled out.

For this reason glueball hunting is a rather complex matter and the understanding of the low meson spectorscopy can only come from an overall comparison between meson production from different dynamical sources, i.e. J/ψ radiative and hadronic decays, $p\bar{p}$ annihilation, hadron induced reactions, $\gamma\gamma$ collisions, high p_T physics, central production etc.

Experiment WA76 at CERN was designed to study centrally produced exclusive final states, and searches for signs of new mesonic states. As the centre of mass energy increases the so called "Double Pomeron Exchange" (DPE) is one of the production mechanisms which is expected to become relatively more important and, if the Pomeron is composed of gluons, DPE can be expected to be a source of gluonium states [1].

A relatively high statistics exclusive study of meson production in all the possible final states in the reactions

$$\pi/p\ p \rightarrow \pi/p\ (X^0)\ p$$

is the physics goal of the WA76 experiment and is carried out here for the first time.

2. The experiment

The WA76 experiment started in 1982 with a run with π^+ and p at 85 GeV/c incident momentum and collected 10^7 events. The physics results presented in this paper come from this run.

A second run has been performed in 1986 with incident protons at 300 GeV/c and collected 1.2 10^7 events. Analysis of this set of data is in progress.

2.1 The run at 85 GeV/c

What are the problems in studying the central production of mesons? The major problem is the large cross sections of diffractive reactions as compared with the DPE reactions. An unbiased study of the reaction $pp \rightarrow p_f (\pi^+\pi^-) p_s$ has been carried out with a bubble chamber exposed to a proton beam of 69 GeV/c [2]. Some results are shown in fig. 1a where the scatter plot of $M^2(p_f\pi^+\pi^-)$ vs. $M^2(p_s\pi^+\pi^-)$ is shown together with its projections. The data clearly show accumulation of events along the two axes indicating the contributions from the forward and backward diffractive production of the $p\pi^+\pi^-$ system with little evidence of a DPE contribution. The cross section for forward diffractive production of the $p\pi^+\pi^-$ system at this energy has been estimated to be $\approx 300\mu b$.

On the other hand, theoretical calculations of the DPE contributions from π and p incident reactions from D.M.Chew and G.F.Chew (fig. 1b) [3], indicate 50 μb for the production of the $(\pi^+\pi^-)$ system via DPE at 85 GeV/c.

This means that, without any selection, the relative rate for the production of diffractive (forward and backward) $(\pi^+\pi^-)$ system with respect to the DPE production, at this energy, is

$$\sigma(\text{diffractive})/\sigma(\text{DPE}) \approx 12/1$$

This calculation does not include other competitive channels other than DPE, i.e. Regge exchanges, Pomeron – Regge exchanges etc.

It is clear that strong selection criteria are needed in order to have a chance to select a really centrally produced system against the large abundance of unwanted diffractive or Regge exchanges contributions. In the following we explain how we solved these problems.

The layout of the Ω spectrometer at CERN used for this experiment is shown in fig. 2.

The positively charged H1 beam (45% p, 47% π^+) in the West Area was incident on a 60 cm long hydrogen target and two Cherenkov counters in the beam allowed positive identification of the pions and protons.

The trigger required:

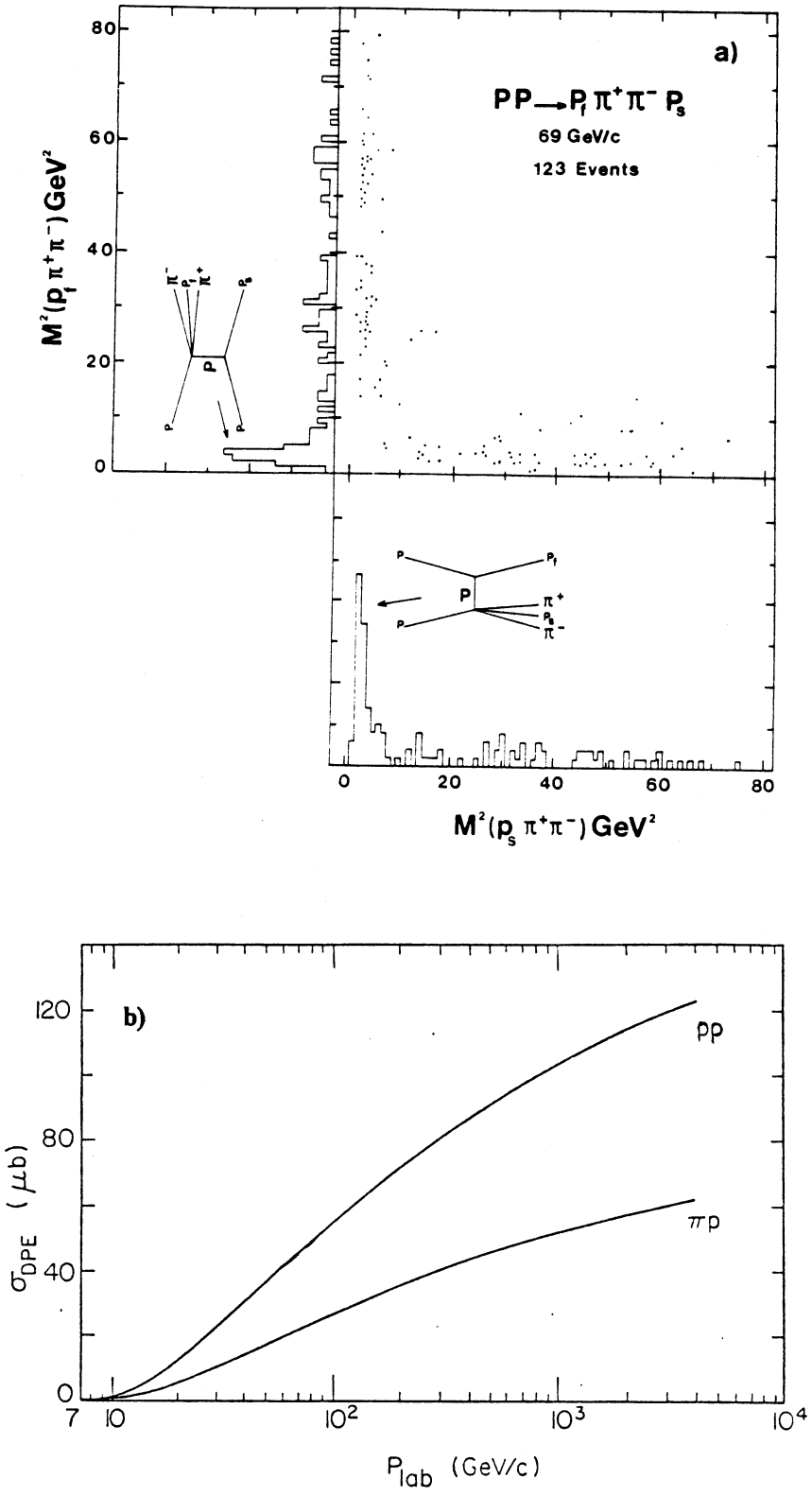

Figure 1: a) Squared ($p_f\pi^+\pi^-$) effective mass vs. squared ($p_s\pi^+\pi^-$) effective mass in the reaction $pp \rightarrow pp\pi^+\pi^-$ at 69 GeV/c from ref.[2]. b) Cross section variation of the DPE cross section as a function of the incident beam momentum for π and p beams, from ref. [3].

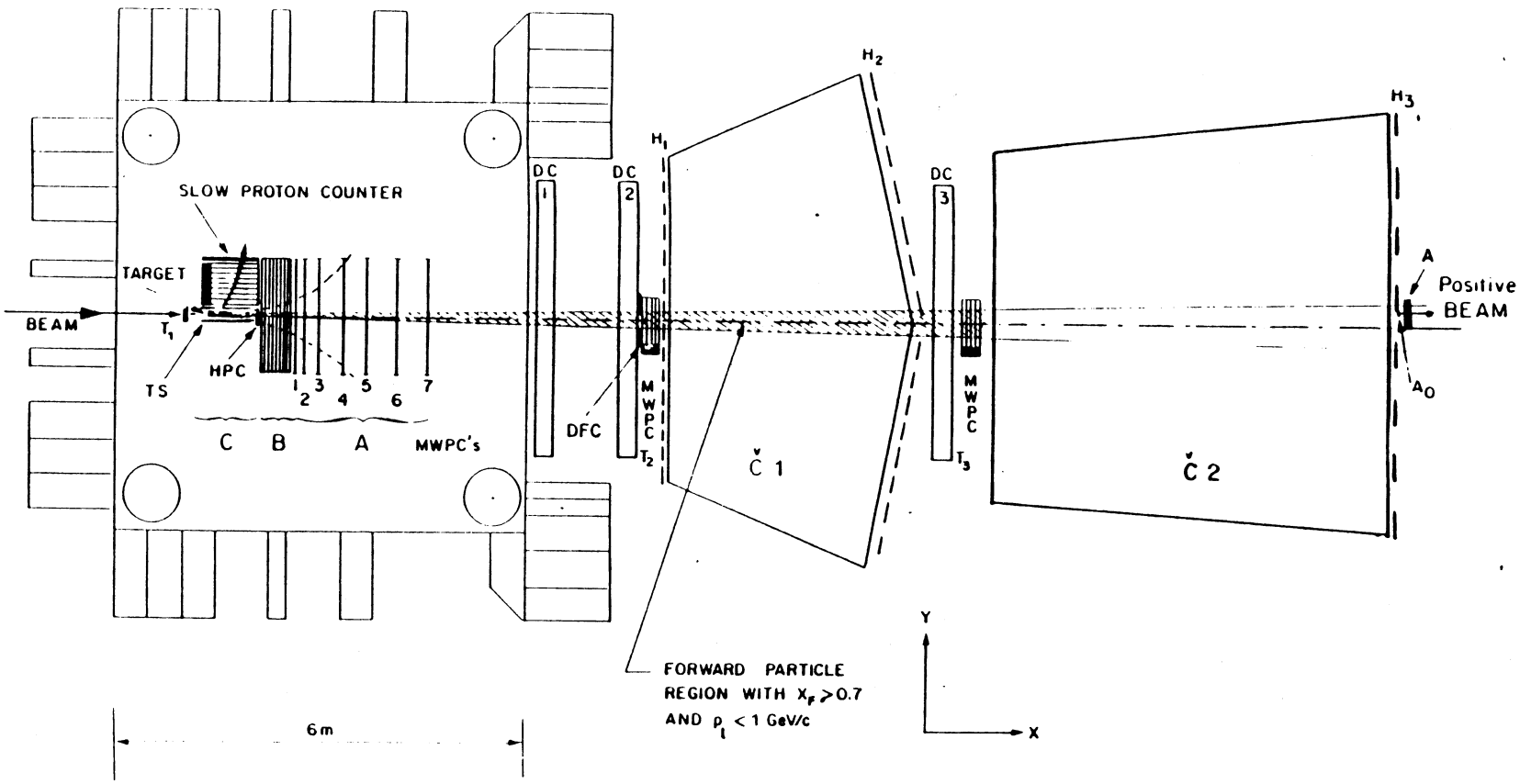

Figure 2: Layout of the CERN Ω spectrometer as used in the WA76 run at 85 GeV/c incident momentum.

1. A fast particle defined by a hit in the counter A (54×60 cm^2) placed after Cherenkov C2, ≥ 1 hit in a single plane of the forward MWPCs T_2 and T_3 and no hit in the beam veto counter A_0;

2. A slow particle defined by demanding one hit on any of the fourteen horizontal slabs of the Slow Proton Counter (SPC), (56×88 cm^2), and ≥ 1 hit on a single plane of the MWPCs situated on one side of the target. In addition, a hit was demanded in the side of the box counter (TS), surrounding the target, which was nearest the SPC.

3. In order to reduce the backward diffraction or excitation we requested no hit in the other three sides of the box TS counter which was left open at its front end to allow particles produced centrally to escape downstream (fig. 3a). The effect of such a selection is visible in fig. 3b where the effective mass $p_s\pi^+$ is shown with no evidence of production of Δ^{++} which is the evidence that the backward diffractive contribution has been almost completely antiselected by the trigger conditions. In addition, the slow particle was identified by means of the pulse-height momentum correlation as shown in fig. 3c.

4. To reduce the forward diffraction or excitation we requested no hit in two counters (DFC) of dimensions (30×60 cm^2) which were placed on either side of the beam and just downstream of drift chamber 2 (DC2). The effectiveness in reducing the forward diffractive contributions was not complete as in the backward side as it can be seen from fig. 3d where a clear Δ^{++} can be seen in the $p_f\pi^+$ effective mass for the p incident data, and $\rho(770)$ and $f_2(1270)$ can be seen in the $\pi^+{}_f\pi^-$ effective mass (fig. 3e) for the π^+ incident data. The diffractive contributions for the reactions $(\pi^+/p)p \rightarrow (\pi^+/p)_f\pi^+\pi^-p_s$, still present in the data and antiselected by software cuts on these forward resonances, resulted in $\approx$45% of the data.

5. Elastic events were vetoed by demanding a forward multiplicity of ≥ 2 (outside the beam region) in one plane of the "A_3" MWPC.

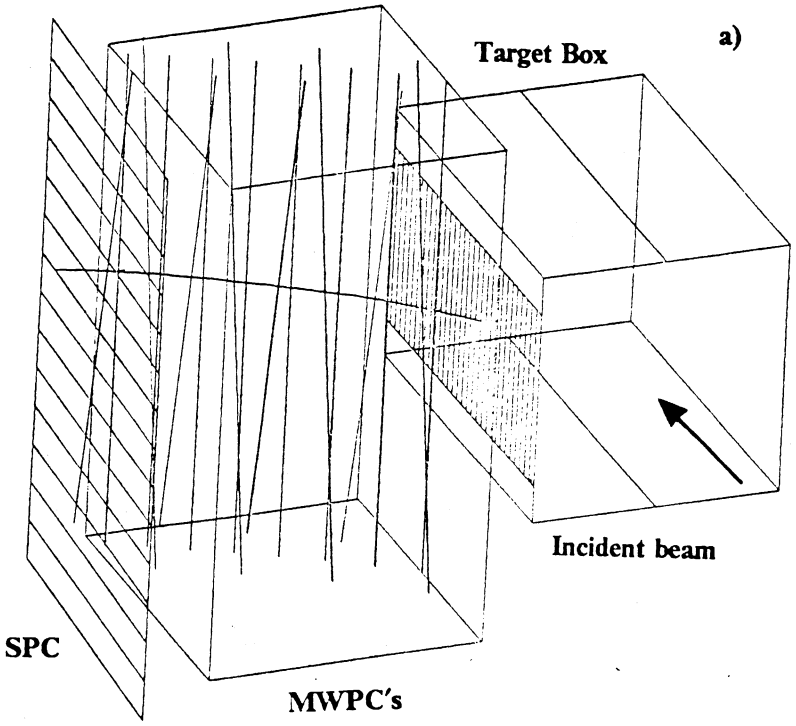

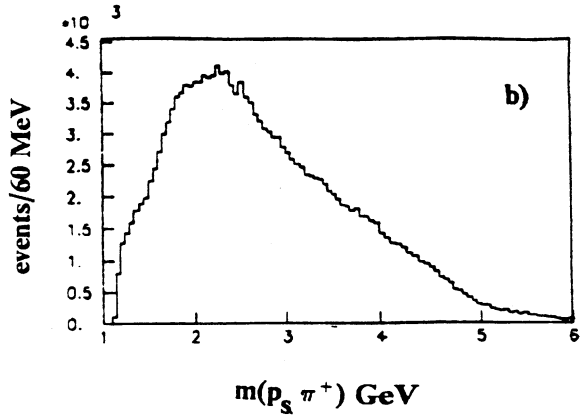

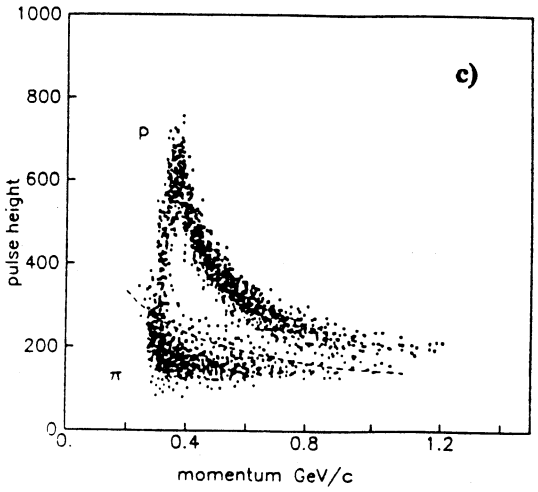

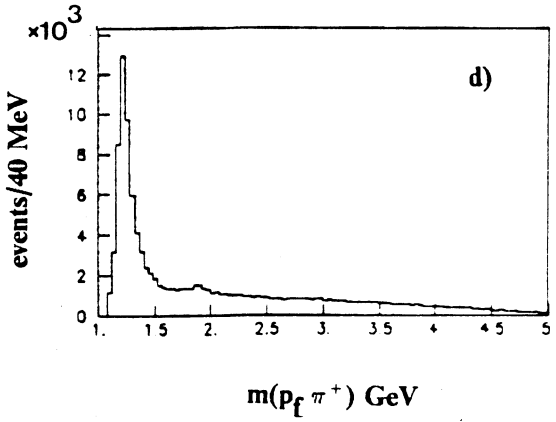

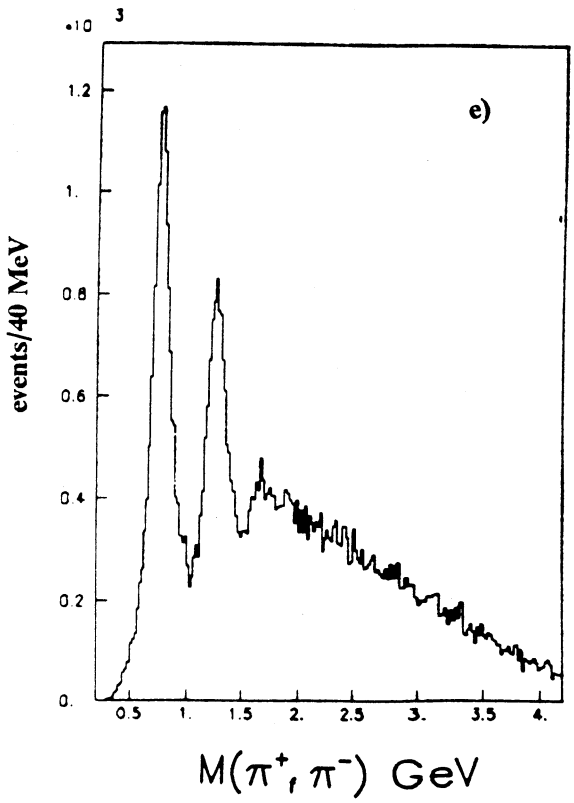

Figure 3: a) WA76 layout in the target region showing respectively, from left to right, the Slow Proton Counter (SPC), the side MWPC's and the target box. The curve indicates a typical slow proton trajectory. b) $p\pi^+$ effective mass; c) Pulse-momentum correlation for the slow particles. The dashed line indicates the p and π regions. d) $p_f\pi^+$ effective mass for incident p beam; e) $\pi^+{}_f\pi^-$ effective mass for π^+ incident beam.

6. In addition to the above conditions (called a π trigger) a K/p trigger was imposed to select events having a negatively or positively charged kaon or proton by demanding correlated hits in the hodoscopes H_1, H_2 and H_3 along with no correlated light in the appropriate region of the multicell Cherenkov counters C1 and C2. An air bag was placed inside C1 in the beam region in order to reduce the multiple scattering on the fast track.

The fast particle momentum , in the 85 GeV/c run, was measured by means of three drift chambers which resulted in a momentum accuracy of ± 1.5 GeV/c at 85 GeV/c.

2.2 The run at 300 GeV/c

The layout used for the run at 300 GeV/c is essentially the same as the one used in the 85 GeV/c run with a few important differences.

1. The beam direction was measured by means of 2 doublets (y and z) of 50μ pitch μ-strips detectors and 2 doublets (y and z) 1/3 mm spacing scintillation counters. The beam momentum bite was held at 0.25%. This allows a very accurate determination of the beam parameters.

2. The outgoing fast particle was measured by means of two sets of 4 planes of 50μ pitch μ-strips detectors placed respectively at 6 m and 10 m from the Ω centre as shown in fig. 4a. The system was set up in such a way that the beam was crossing only two offset y planes in order to have a constant calibration of the exact position of the μ- strips planes. An example of the raw hit distribution on the offset plane of the 6 m μ-strips is shown in fig. 4b. This layout was also automatically antiselecting the elastic events. The precision obtained with this system has been estimated by measuring the momentum of beam tracks by using of the first beam μ-strips and the forward μ-strips planes and is ± 2.7 GeV/c at 300 GeV/c (see fig. 4c).

   A typical event is shown in fig. 5a (charged) and 5b (neutral). The fast track, which is not seen by the MWPCs and DC's, is measured by using the vertex coordinates (determined very accurately in y and z by the beam) and the two μ-strips points at 6 m and 10 m.

3. The Ω γ detector was placed after Cherenkov 2 to detect γ, π^0 and η.

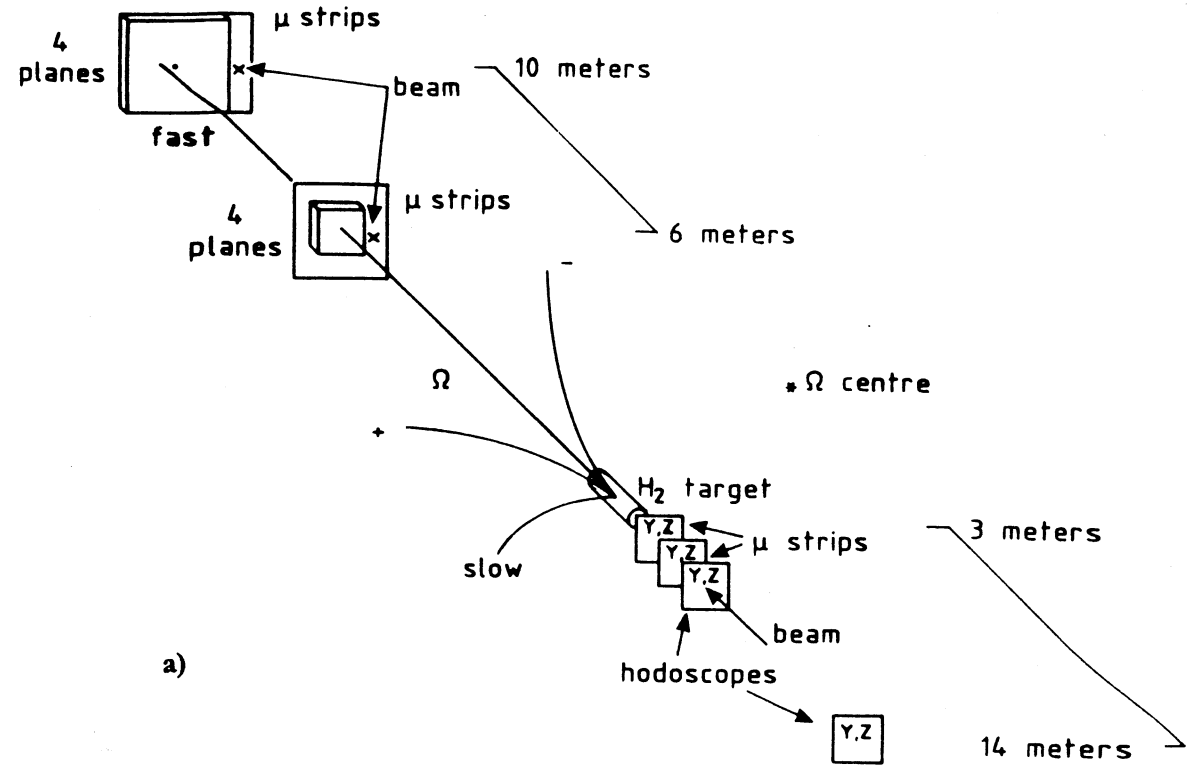

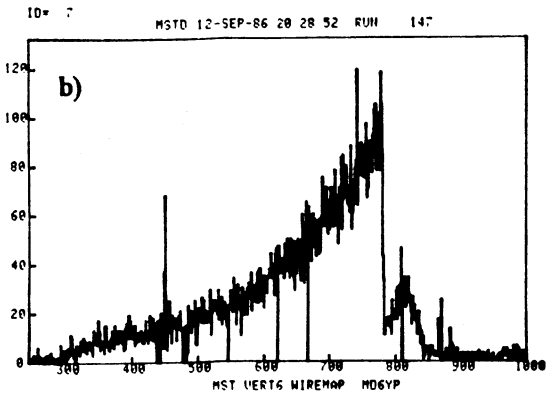

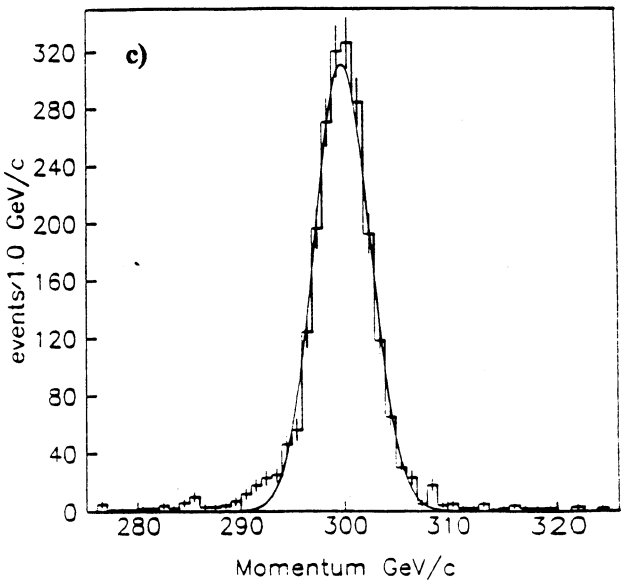

Figure 4: a) Layout of the μ-strips and scintillators used to measure the beam and the fast particle in the WA76 run at 300 GeV/c. b) Raw hits on the shifted μ-strip at 6m from the Ω centre; c) Beam momentum determination for the calibration of the alignment of the whole system. The curve represents a gaussian fit to the data.

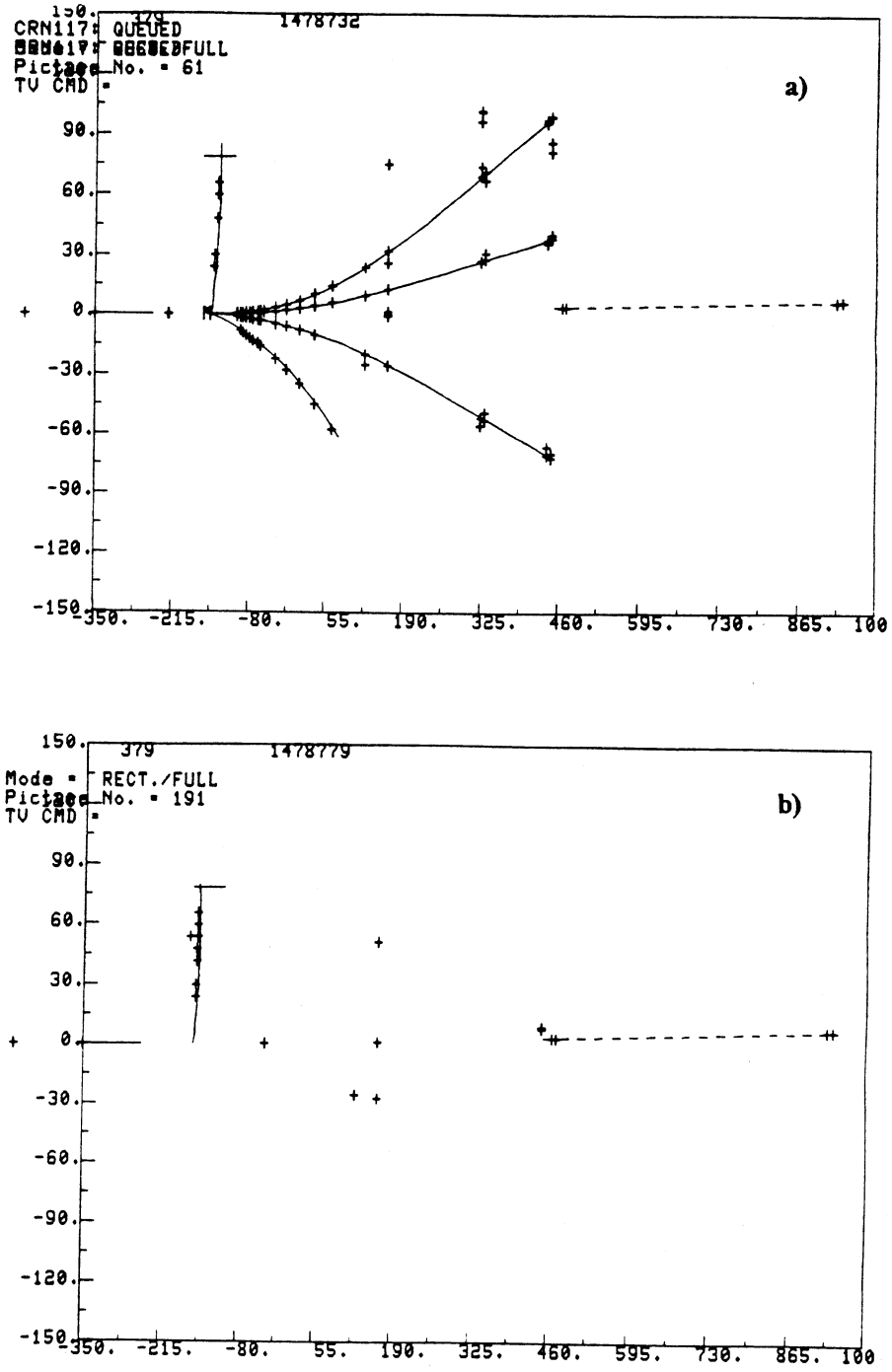

Figure 5: Typical events at 300 GeV/c. From left to wright are shown the beam μ-strips, the MWPC's, the Drift Chambers and the forward μ-strips. The dashed line indicates the reconstructed track in the forward μ-strips. a) Six outgoing charged tracks event; b) two charged and neutrals.

3. Physics at 85 GeV/c

The 85 GeV/c data have been analyzed, several results have been published and the study of a few channels is still in progress. As explained in chapter 2, the trigger selected the class of graphs shown in fig. 6a, i.e. double exchanges graphs with no possibility, due to the limited rapidity gap between the fast and slow particles and the central system, at this energy, to isolate DPE from other exchanges mechanisms. A typical distribution of x – Feynman for the slow, the central system and the fast particle are shown in fig. 6b.

3.1 Isolation of the reaction $\pi^+/p\ p \rightarrow \pi^+/p\ (X^+\ X^-)\ p$

The reactions

$$\pi^+/p\ p \rightarrow \pi^+/p\ (X^+\ X^-)\ p \text{ , where } X = \pi, K, p$$

have been isolated from the sample of events having four outgoing tracks. Fig. 7a shows the total missing P_t where a clear signal is evident from candidate "4C" events. Fig. 7b shows the resulting missing P_x distribution after requiring P_t cuts. The above plots show that the momentum balance events can be clearly isolated at this energy. The energy balance can be written as:

$$(\pi^+/p)_i\ p \rightarrow (\pi^+/p)_f\ p_s\ X^+_1\ X^-_2$$

$$E_i + m_p = E_f + E_s + \sqrt{(p^2_1 + m^2)} + \sqrt{(p^2_2 + m^2)}$$

equation which can be solved directly for m^2. The m^2 distribution for all the data is shown in fig. 7c and is dominated by a large peak at the squared π mass and is the signal of the reaction having the $\pi^+\pi^-$ system in the final state. Two smaller peaks are also seen at the squared K and p masses which indicate the presence of the K^+K^- and $p\bar{p}$ final states.

A different spectrum is obtained by requiring one particle to be identified as a K or K/p by the Cherenkov system and the other, if reaching the Cherenkov system, to have a mass identification compatible with the K hypothesis (see fig. 7d). In this case the π peak is considerably reduced and clear signals of the K^+K^- and $p\bar{p}$ reactions can be seen. The latter final states can also be isolated with little background.

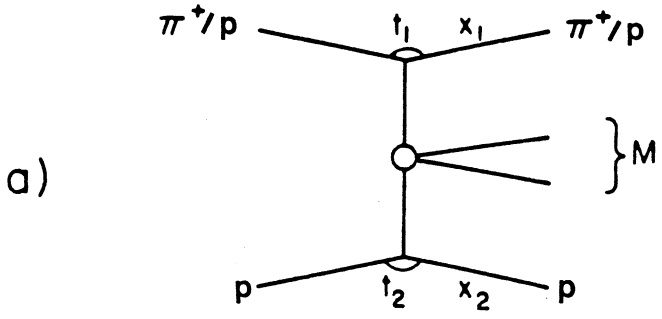

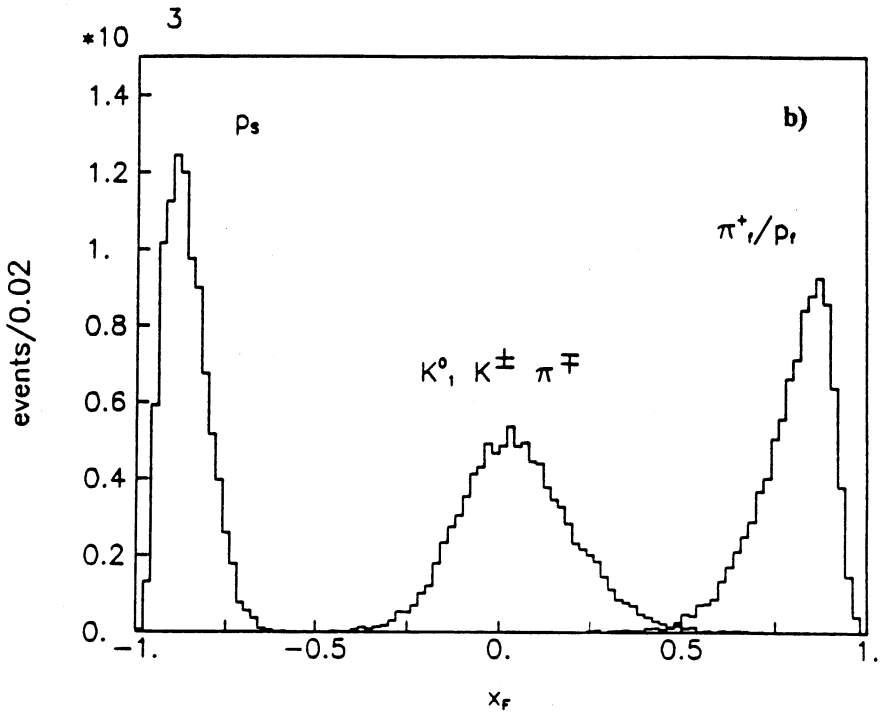

Figure 6: a) Feynman graph selected by the WA76 trigger conditions; b) Typical $x_{Feynman}$ distributions as selected by the trigger conditions. The x_F of the slow proton, the central system and the fast particle respectively are shown.

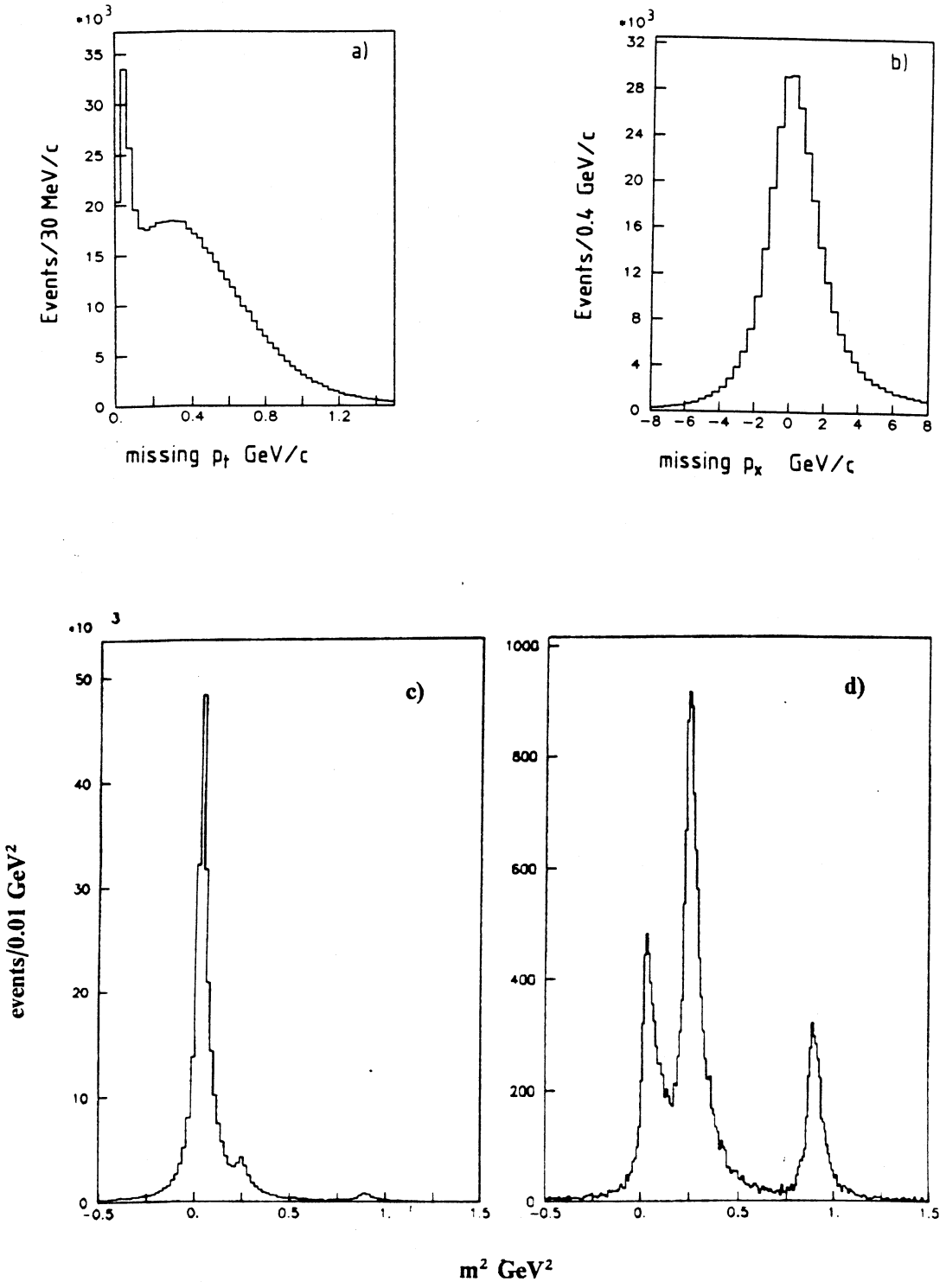

Figure 7: a) Missing transverse momentum distribution for events with four outgoing tracks; b) Missing longitudinal momentum after P_t cut. c) Ehrlich mass distribution for all the events and d) after having used the Cherenkov information to select the centrally produced $K^+ K^-$ final state.

4. Some dynamics from the Central Region

The dynamics and the processes underlying the central production of mesons are largely unknown and it is of interest to find possible hints of the dynamical sources of meson production. Some interesting features have been observed.

1. Fig. 8c shows the centrally produced K^+K^- mass spectrum as obtained in the WA76 experiment at 85 GeV/c [4]. It is interesting to compare this spectrum with the K^+K^- mass spectrum coming from two different sources: incident π^- [5] (fig. 8a) and incident K^- [6] (fig. 8b). These spectra clearly show resonance production influenced by the nature of the incident beam, i.e. the π^- spectrum shows resonances coupled to non − strange quarks ($f_0(975)$, $f_2(1270)/a_2(1320)$, etc.), while the K^- induced spectum shows resonances coupled to strange quarks ($\phi(1020)$, $f'_2(1525)$). It can be seen the the spectrum of fig. 8c shows, in the low mass region, all these resonances together, indicating a "flavour blind" production mechanism, i.e. resonances coupled to strange and non − strange quarks are produced in the central region with similar strength.

2. The study of channels with 4 or 5 particles in the final states enables a search for associated resonance production to be made. Evidence has been found for $\phi\phi$ production in the study of $2K^+2K^-$ final state [7] (fig. 9a), $K^{*0}\ \bar{K}^{*0}$ in the $K^+K^-\pi^+\pi^-$ final state [8] (fig. 9b) and probably $\phi\omega$ in the $K^+K^-\pi^+\pi^-\pi^0$ final state (fig. 9c). It should be noticed that in the 85 GeV/c run the π^0 where not detected so they were reconstructed only as missing particles. This implies that channels using π^0's are affected by uncertienties due to the bad experimental resolution. The $\phi\phi$ and $K^*\bar{K}^*$ effective mass distributions are shown in fig. 9d and 9e and show accumulations near threshold.

3. Ref. [9] has found an anomalous high $\phi\phi$ production in π^- induced reactions at 23 GeV/c: $\sigma(\phi\phi)/\sigma(\phi K^+K^-)\approx 0.2$ and it has been suggested [10] that a large $\phi\phi$ production with respect to ϕ K K production in π induced reactions is evidence of intermediate gluonic bound states. The study of the centrally produced $2K^+2K^-$ gives the largest ever observed production of $\phi\phi$: $\sigma(\phi\phi)/\sigma(\phi K^+K^-)\approx 0.7$.

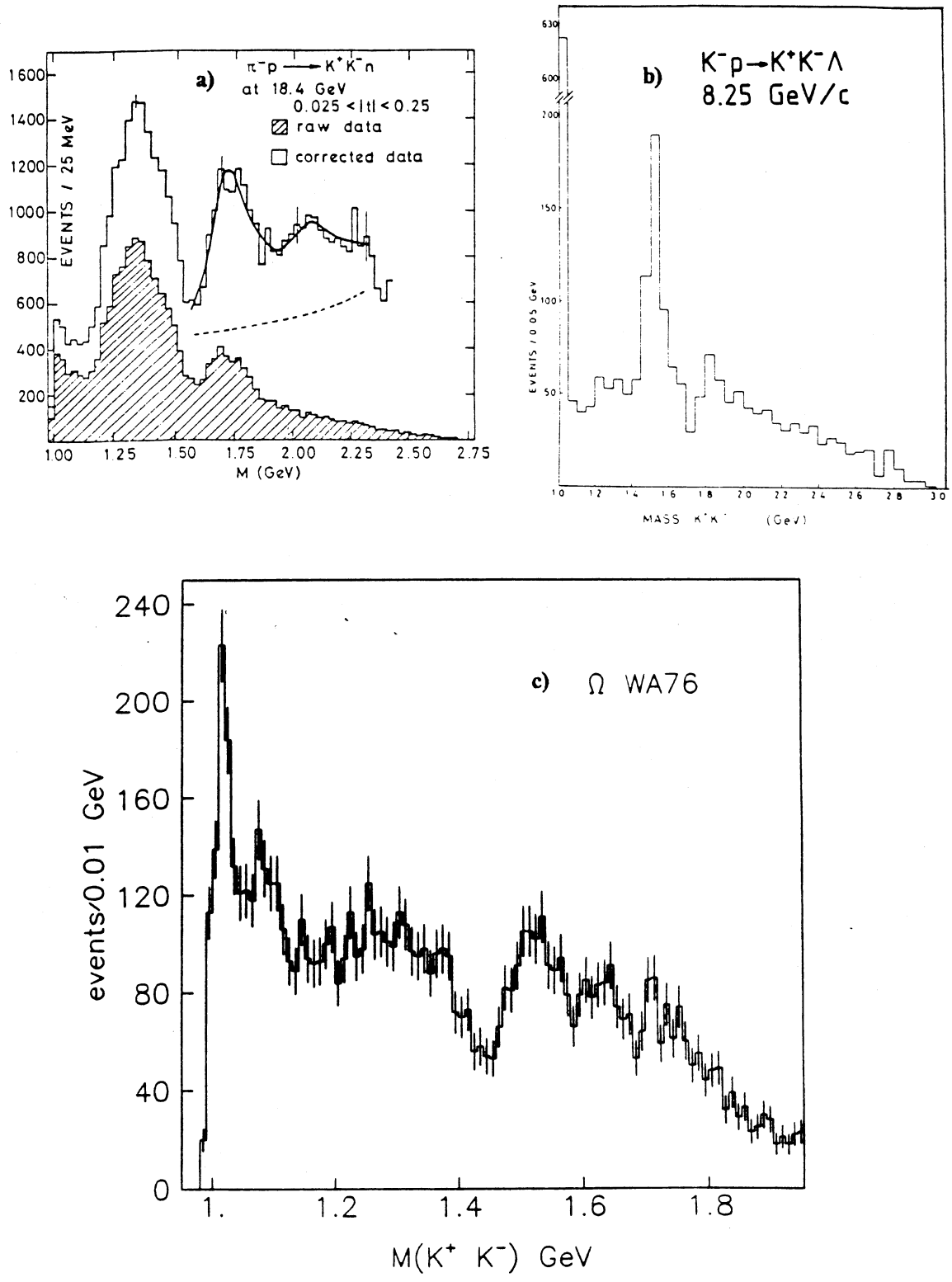

Figure 8: a) K^+K^- effective mass from incident π^- beam [5]. b) K^+K^- effective mass from incident K^- beam [6]. c) Centrally produced K^+K^- effective mass from WA76.

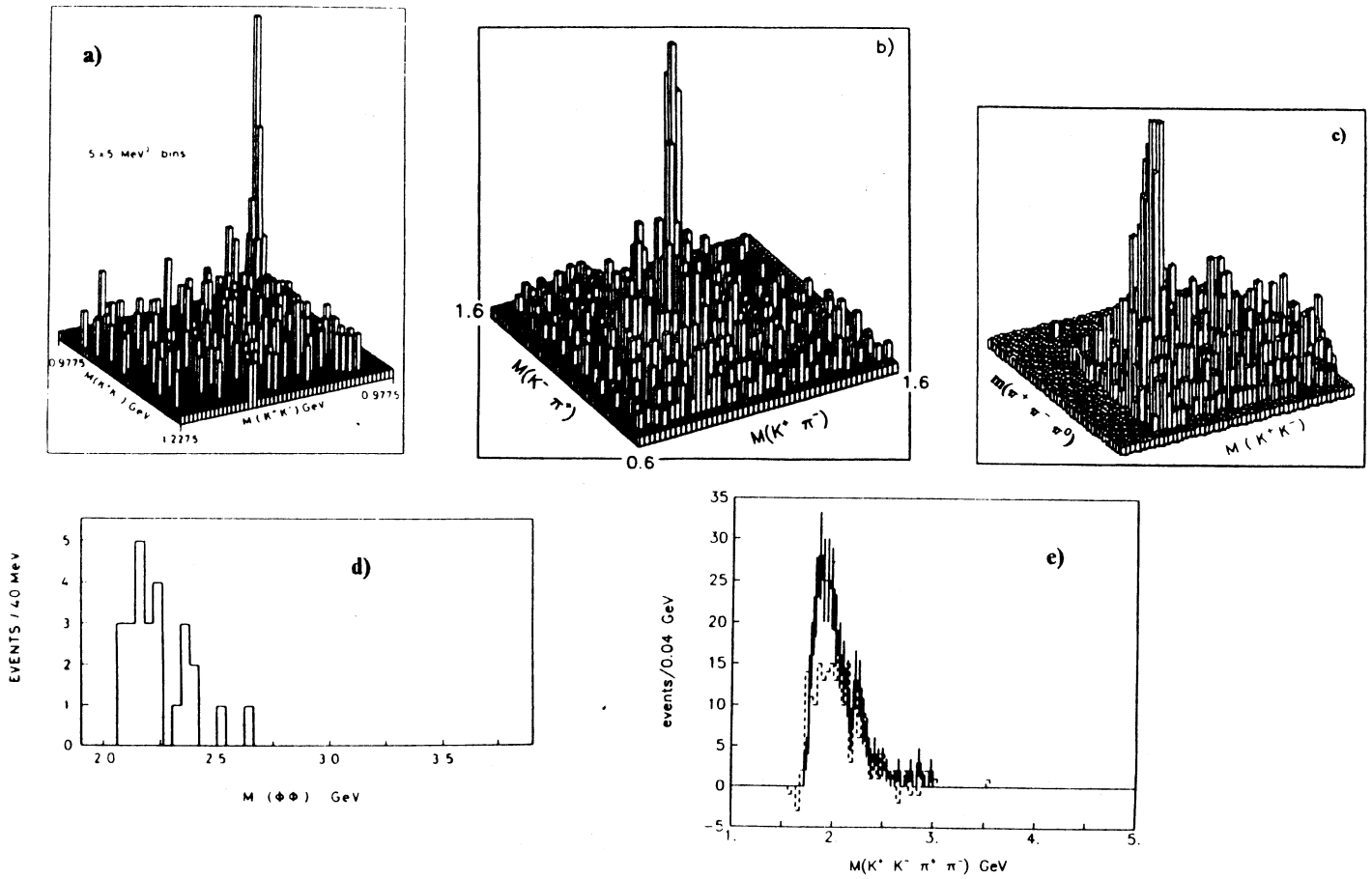

Figure 9: Results from the WA76 study of associated vector meson production in the central region. a) Lego plot $m(K^+K^-)_{1,2}$ vs. $m(K^+K^-)_{3,4}$ from the reaction $\pi^+/p\ p \rightarrow \pi^+/p\ (2K^+2K^-)\ p$; b) Lego plot $m(K^-\pi^+)$ vs. $m(K^+\pi^-)$ from the reaction $\pi^+/p\ p \rightarrow \pi^+/p\ (K^+K^-\pi^+\pi^-)\ p$; c) Lego plot $m(\pi^+\pi^-\pi^0)$ vs. $m(K^+K^-)$ from the reactions $\pi^+/p\ p \rightarrow \pi^+/p\ (K^+K^-\pi^+\pi^-\pi^0)\ p$; d) $\phi\phi$ effective mass; e) $K^{*0}\ \bar{K}^{*0}$ effective mass. The dashed histogram represents the $K^{*0}\ K\pi$ background.

It is not clear, at present, how to interpret these experimental observations. One possibility is that gluons, as well as quarks, are interacting in the central region in order to produce the observed features.

5. The search for the 0^{++} glueball

Calculations of the glueball spectrum in QCD indicate the possibility that the lightest glueball should have $J^{PC} = 0^{++}$ and have a mass around 1 GeV [11]. If it is below the $K\bar{K}$ threshold it can only decay into pions so it should be present in $\pi\pi$ scattering data.

Recently, a multichannel analysis has been performed on different $\pi\pi$ and $K\bar{K}$ data but mostly based on CERN ISR (Axial Field Spectrometer (AFS) Collaboration [12]) data coming from the DPE reactions $pp \to pp\pi^+\pi^-$ abd $pp \to ppK^+K^-$. The $\pi^+\pi^-$ mass spectrum is shown in fig. 10a and is characterized by a threshold enhancement and a sharp drop around the $K\bar{K}$ threshold, while the $K\bar{K}$ mass spectrum from the same experiment is shown in fig. 10b. The analysis of ref. [13] interpreted the so called "S^* effect" as due to the presence of two states,

$S_1(993)$ with $E_R = 0.993 - 0.023i$ GeV, $g_\pi = 0.23$, $g_K = 0.28$

$S_2(988)$ with $E_R = 988$ GeV , $g_\pi \approx 0$, $g_K = 0.35$

where E_R is the position of the complex pole, g_π and g_K describing the $\pi\pi$ and $K\bar{K}$ couplings of the two resonances. The $S_1(993)$ is roughly equally coupled to $\pi\pi$ and $K\bar{K}$ and is interpreted as a possible scalar gluonium state. The $S_2(988)$, coupled only to $K\bar{K}$, is interpreted as a pure $s\bar{s}$ state or a $K\bar{K}$ molecule.

The WA76 data, summed over the two incident (π^+ and p) beams but split into two different t regions (t is the sum of t_1 and t_2, the four momentum transfer at the upper and the lower vertex respectively in the diagram shown in fig. 6a) are shown in fig. 10c,d. The low t region shows similar features to the AFS data, i.e. a threshold enhancement and a drop at the $K\bar{K}$ threshold. The high t region, on the other hand, shows clear ρ and f_2 structures and a shoulder in the 0.94 GeV region. The total spectrum is shown in fig. 11a.

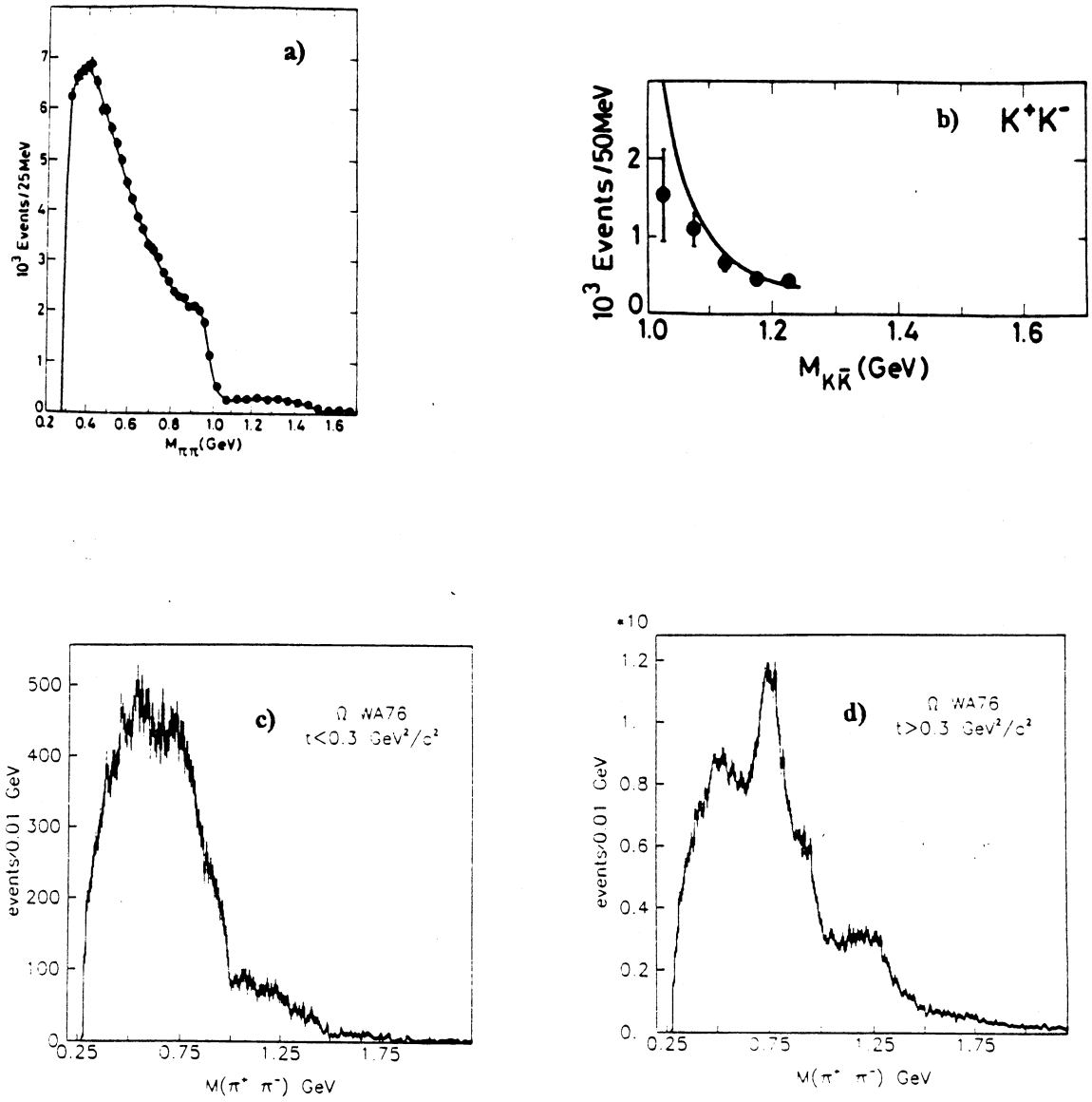

Figure 10: a),b) $\pi^+\pi^-$ and K^+K^- effective mass distributions from ref. [13]. The curves show projection of the multichannel fit. c),d) $\pi^+\pi^-$ effective mass from WA76 for $t < 0.3$ GeV^2/c^2 and $t < 0.3$ GeV^2/c^2 respectively.

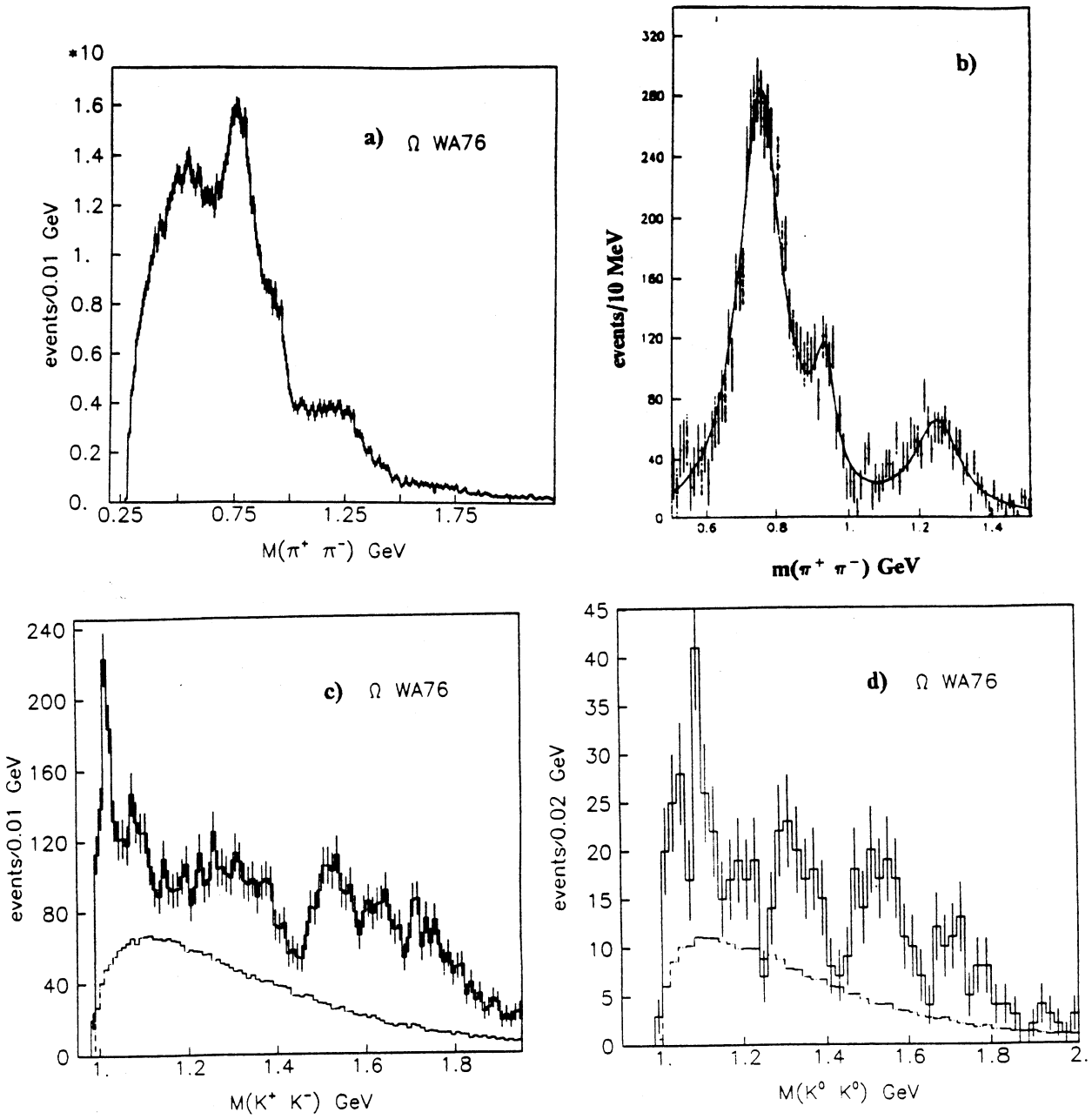

Figure 11: a) Total $\pi^+\pi^-$ effective mass from WA76; b) Preliminary fit of the π^+ incident data after background subtraction. c),d) K^+K^- and $K^0\bar{K}^0$ effective mass from WA76. The dashed histograms shows the estimated phase space from mixed events, the normalization is arbitrary.

One way to parametrize an object coupled to different decay channels is the Flatte' formulation [14] which has a very simple mathematical expression

$$\sigma_{\pi,K} \alpha \frac{m_s \Gamma_\pi}{m^2_s - m^2 - i m_s(\Gamma_\pi + \Gamma_K)}$$

where $\Gamma_\pi = g_\pi q_\pi$ and $\Gamma_K = g_K q_K$. The fit of the π^+ incident data, in the WA76 experiment, with the above parametrization is shown in fig. 11b after background subtraction. The K^+K^- and $K^0\bar{K}^0$ mass spectra are shown in fig. 11c,d. The two spectra show similar features with evidence of a large number of structures, in particular a threshold enhancement is visible in both spectra. In order to visualize the phase space contribution in both spectra the combinatorial phase space obtained by taking kaons from different events is plotted. Whether the structure seen in the $\pi\pi$ mass spectrum around 0.94 GeV and the threshold enhancement observed in the $K\bar{K}$ projection belong to a single or two resonances is not clear. The analysis of these channels is still in progress.

An inspection of the high mass region of both the K^+K^- and $K^0\bar{K}^0$ mass spectra show structure above the $f'_2(1525)$ which have been shown [4] not associated to the g meson (in the $K^0\bar{K}^0$ mass spectrum that is forbidden because only even spins are allowed). The K^+K^- mass spectrum, in addition, suggests the presence of two resonances in this region. The fit is shown in fig. 12a and gives the following parameters,

$$m_1 = 1629 \pm 10 \text{ MeV} \quad \Gamma_1 = 82 \pm 30 \text{ MeV}$$

and

$$m_2 = 1742 \pm 10 \text{ MeV} \quad \Gamma_2 = 127 \pm 30 \text{ MeV}$$

For comparison, fig. 12b,c,d show the K^+K^- mass spectra recoiling against γ, ω and ϕ in the J/ψ decay [15]. The first two mass spectra show structure in the region of the θ with parameters $m(\theta) = 1720 \pm 10 \pm 10$ MeV and $\Gamma(\theta) = 130 \pm 20$ MeV while an incoherent fit of the K^+K^- mass spectrum recoiling against the ϕ gives the values $m = 1671 \pm 15 \pm 10$ MeV and $\Gamma = 126 \pm 50 \pm 15$ MeV. If we are observing the same structures, the mass and widths of the structures observed in the J/ψ decay are consistent with the ones measured in the WA76 experiment.

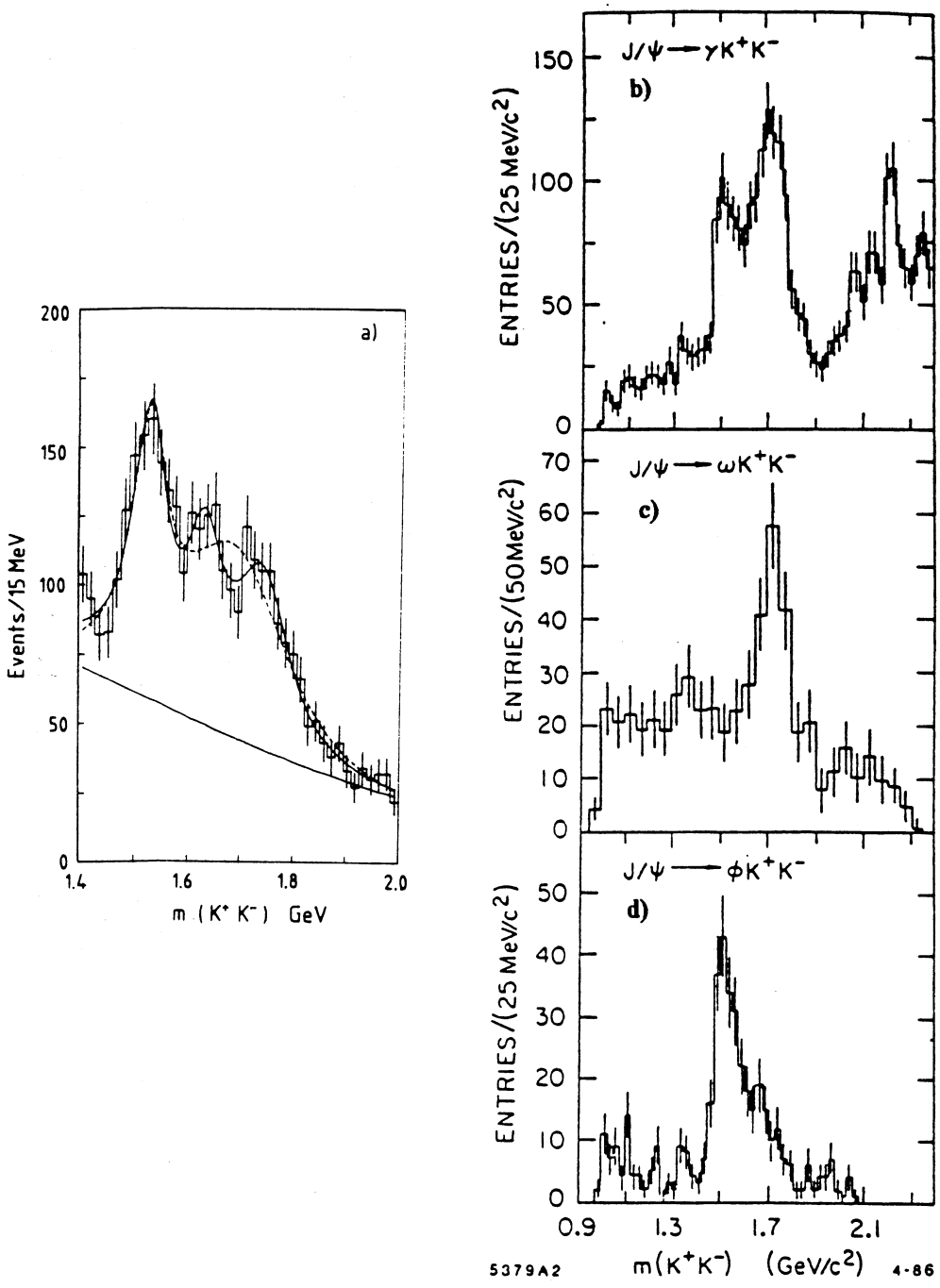

Figure 12: a) Fit of the WA76 K^+K^- mass spectrum in the high mass region. b),c),d) K^+K^- effective mass distribution recoiling against γ, ω and ϕ respectively in the J/ψ decay.

6. The E/ι puzzle

The E/ι puzzle can be summarized as follows. One, two, three or even more states are observed decaying to $K\bar{K}\pi$ and/or $\eta\pi\pi$ in the mass region around 1.4 GeV which some experiments find to have $J^{PC}=0^{-+}$ (ι) while others find $J^{PC}=1^{++}$ (E). The interest in this region is that, if $J^{PC}=0^{-+}$, the resonance could be a glueball candidate while, if $J^{PC}=1^{++}$, it can be a normal $q\bar{q}$ object.

For a recent review of the subject see ref. [16]. The experimental situation can be summarized as follows:

1. A pseudoscalar state, $J^{PC}=0^{-+}$, is observed in the radiative J/ψ decay [17] and $p\bar{p}$ annihilation at rest [18] and is not seen together with the $f_1(1285)$, an established axial vector state. In both reactions the $\delta\pi$ decay mode seems to be important. The state seen in the J/ψ decay has a mass of ≈1460 MeV and a width of ≈100 MeV. In contrast the state seen in $p\bar{p}$ annihilation has a mass of 1425±7 and a width of 80±10 MeV However the state seen in the radiative J/ψ decay looks more like a superposition of more than one state since a simple Breit−Wigner is not enough to describe the mass spectrum. In addition the existence of a $\delta\pi$ decay mode is not supported by the analysis of radiative decay of the J/ψ to $\eta\pi\pi$.

2. Two experiments [19,20] find evidence for a pseudoscalar state at the E mass (≈1420 MeV) in the study of the $K\bar{K}\pi$ and $\eta\pi\pi$ systems in π^- induced reactions at 8 GeV/c. However, this results is in contradiction with a previous, lower statistics, bubble chamber experiment [21] which found 1^{++} as quantum numbers of the same object. The study of the $\eta\pi\pi$ system revealed also the existence of a new pseudoscalar particle in the $f_1(1285)$ region, the η(1275). These observations are not supported by the study of γγ collisions where these states, if belonging to the radial excitation sector, should clearly appear [22].

3. The axial vector state E (1^{++}) is generally observed together with the $f_1(1285)$, has $K^*\bar{K}$ as dominant decay mode, a mass of 1425 MeV and a width of ≈60 MeV. This state has been seen in π^- induced reactions [21], in the WA76 experiment [23], in γγ collisions [24] and in the hadronic decay of the J/ψ to $\omega K\bar{K}\pi$ [25]. The data from the WA76 experiment are shown

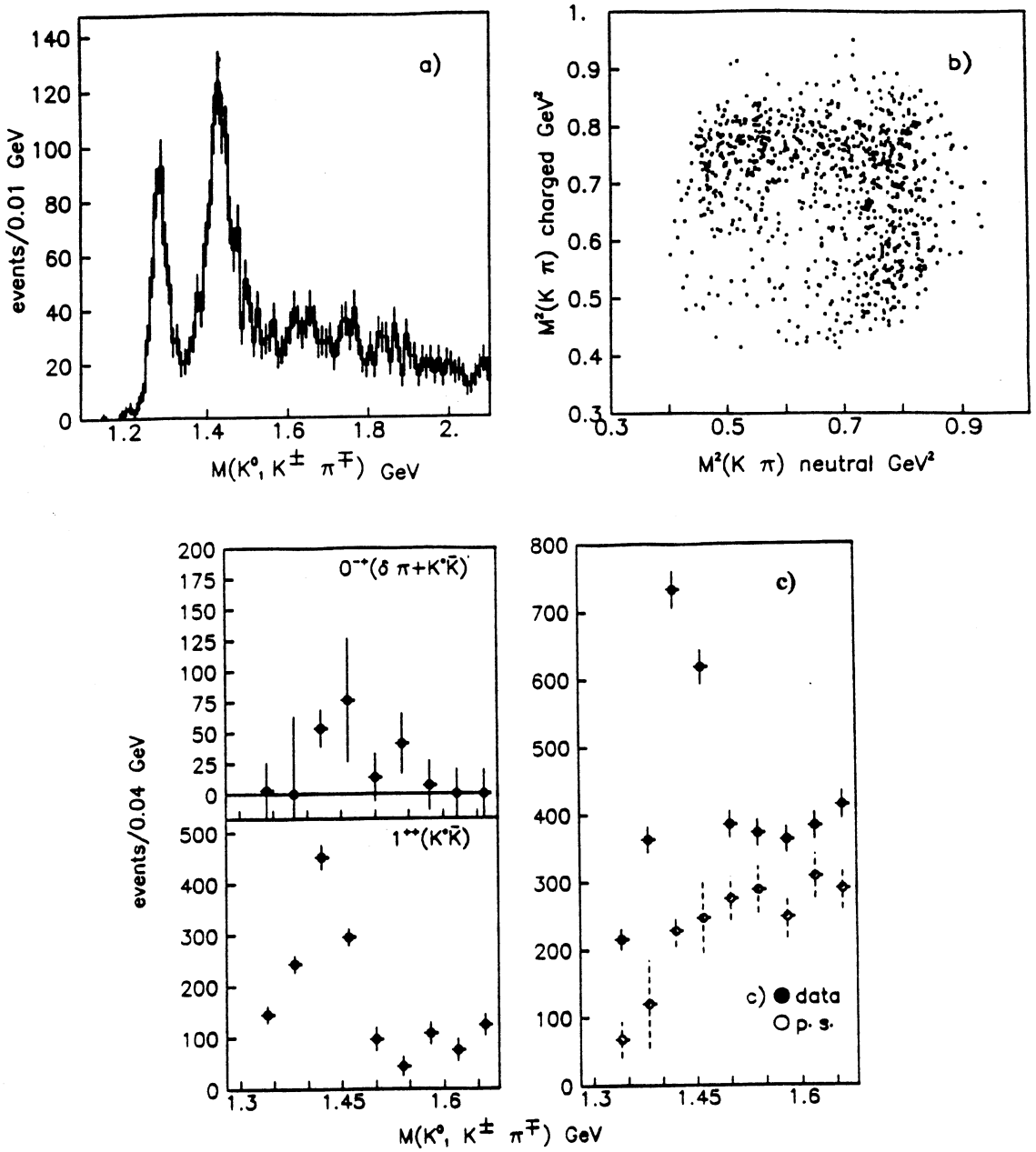

Figure 13: a) $K^0{}_1K^{\pm}\pi^{\mp}$ centrally produced mass spectrum from incident π^+ and p at 85 GeV/c by using the CERN Ω spectrometer b) Dalitz plot, c) Results from Dalitz plot analysis.

in fig. 13 which contains the mass spectrum, the Dalitz plot showing clear K^* bands from the low background E signal and the results of the Dalitz plot analysis which shows a large ($\approx$86%) 1^{++} component and a small 0^{-+} component.

4. A new axial vector state, D′(1526) having a mass of 1526±6 MeV and a width of 107±15 MeV has been observed by two experiments [26,27] in the analysis of the $K\bar{K}\pi$ system from K^- induced reactions.

Too many pseudoscalars and axial vector mesons are present in this mass region to be understood in terms of a simple quark model. As usual more high statistics data are needed in order to help clarify the situation.

7. The a_1 problem

The a_1 resonance, having $J^{PC} = 1^{++}$, is still a puzzle for light meson spectroscopy. Its existence seem settled by two large experiments which studied the 3π system in diffractive and charge exchange reactions [28,29] and extracted the signal from a large Deck background. The mass and width were determined to be respectively $m(a_1)$ = 1275±28 MeV and $\Gamma(a_1)$ = 316±45 MeV.

A different a_1 has been found in backward production of the charged 3π system in the reacion $K^-p \to \Sigma^-\pi^+\pi^+\pi^-$ at 4.15 GeV/c [30]. Here mass and width were found to be 1041±13 MeV and 230±50 MeV respectively.

Recent data from τ decay $\tau \to 3\pi\nu_\tau$ where the full 3π mass spctrum is assumed to belong to the a_1 resonance find quite different results. Three experiments find respectively 1056±20 MeV [31], 1194±14 MeV [32] and 1046±11 MeV [33] for the a_1 mass and a quite large width of the order of 500 MeV.

A contribution to the a_1 problem also comes from the WA76 experiment via the study of the centrally produced $2\pi^+2\pi^-$ system. The 4π mass spectrum is shown in fig. 14a and shows a clear structure at the $f_1(1285)$ mass. A fit which includes the reflections coming from the η' and D from the $\eta\pi\pi$ system where a slow π^0 is not detected gives the following paramaters for the mass and width:

$$m = 1280 \pm 2 \qquad \Gamma = 39 \pm 15 \text{ MeV}$$

The study of the 3π system in the 4π final state is made complex by the presence of a combinatorial background, i.e. in the three pion mass spectrum 3 entries are combinatorials and only one entry is physics. In order to remove the combinatorial background the method of mixed events has been used. Artificial events have been generated where each of the four pions was taken from a different event. The resulting 3π mass spectrum from this kind of Monte – Carlo events was normalized to be 3/4 of the total. The true spectrum as well as the combinatorial one is shown in fig. 14b. The data show structure in the a_2 region and suggest a wide structure peaking above 1.0 GeV. The subtracted spectrum is shown in fig. 14c and clearly suggest the presence of two resonance structures. The subtracted spectrum has been fitted by using two simple Breit – Wigner shapes one being the standard $a_2(1320)$ the other giving the following values:

$$m = 1022 \pm 20 \text{ MeV} \quad \Gamma = 277 \pm 50 \text{ MeV}$$

in good agreement with the values quoted in ref. [30] for the backward a_1 production by incident K^-.

In order to test if the method used to estimate the combinatorial background is biasing the data or generating false peaks, the same method has been applied to the $\pi^+\pi^-$ mass distribution which also suffers from combinatorial problems af the sime type as the 3π spectrum. The results are shown in fig. 14d where the raw 2π mass spectrum is shown together with the subtracted one. Clear structure can be seen at the ρ and f_2 masses with some indication of K^0. No artificial structure seems to be generated in this mass spectrum.

We have attempted a Dalitz plot analysis of the 3π spectrum as a function of the mass. Preliminary results of this analysis are shown in fig. 15. The $a_2(1320)$ signal is clearly seen in the 2^+ $\rho\pi$ amplitude. The 1^+ amplitudes show different behaviour: the 1^+ $\varepsilon\pi$ amplitude has a threshold enhancement and gradually decreases as the $\rho\pi$ amplitude increases. Their sum is also shown in fig. 15 and shows a large structure having a maximum in the same region as the mass spectrum. The other waves (not shown) have only a phase space behaviour.

Whether these data show evidence for an a_1 resonance is a matter for further investigation.

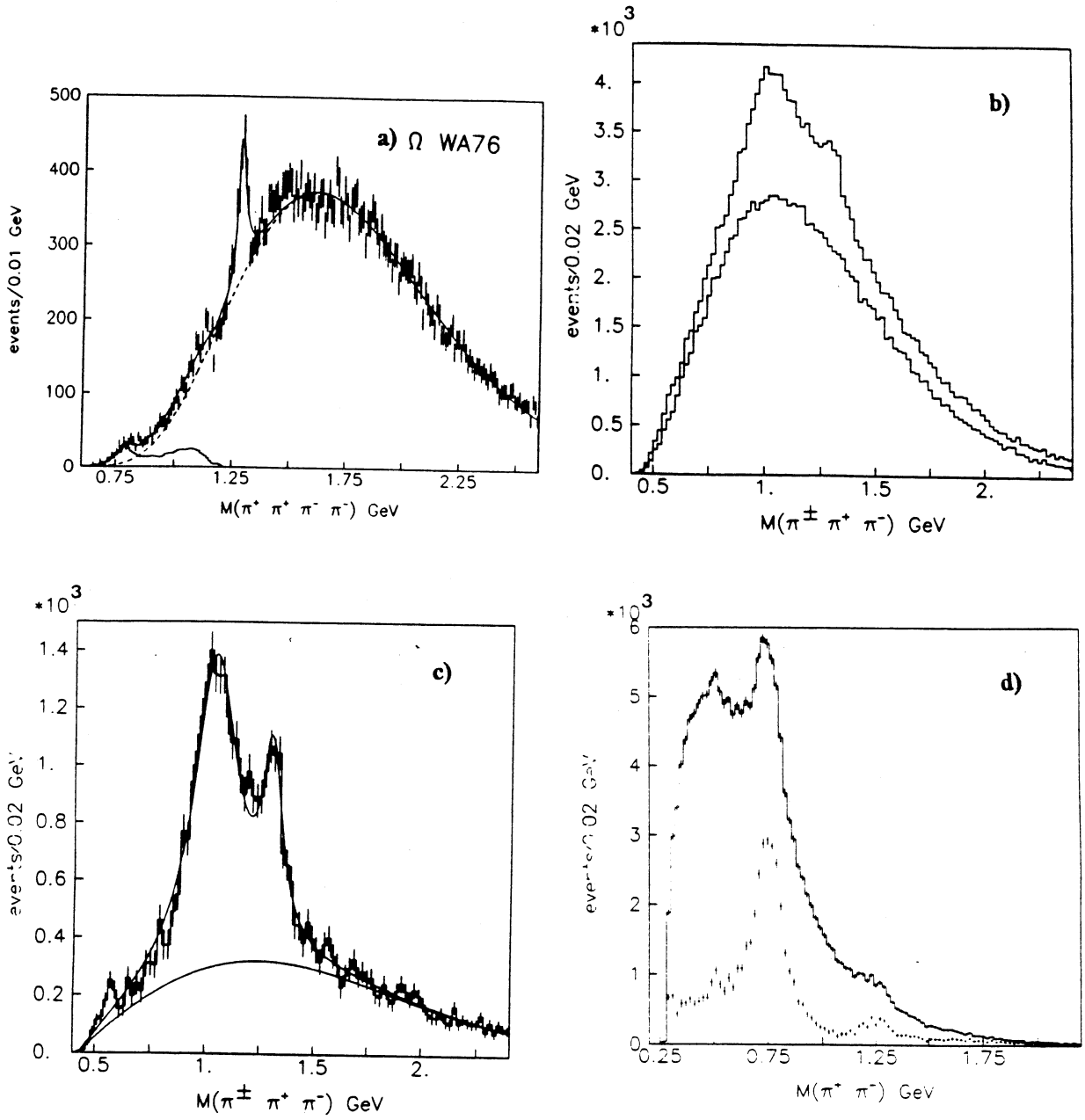

Figure 14: a) Centrally produced $2\pi^+2\pi^-$ effective mass distribution from WA76. The line is the result of the fit described in the text. b) 3π effective mass distribution (4 entries per event). The lower histogram shows the combinatorial background estimated by using the method of mixed events and normalized to 3/4 of the total entries. c) 3π effective mass after subtraction of the combinatorials. The line is the result of the fit described in the text. d) $\pi^+\pi^-$ effective mass in the same reaction. The same figure shows the result of subtracting the combinatorial background.

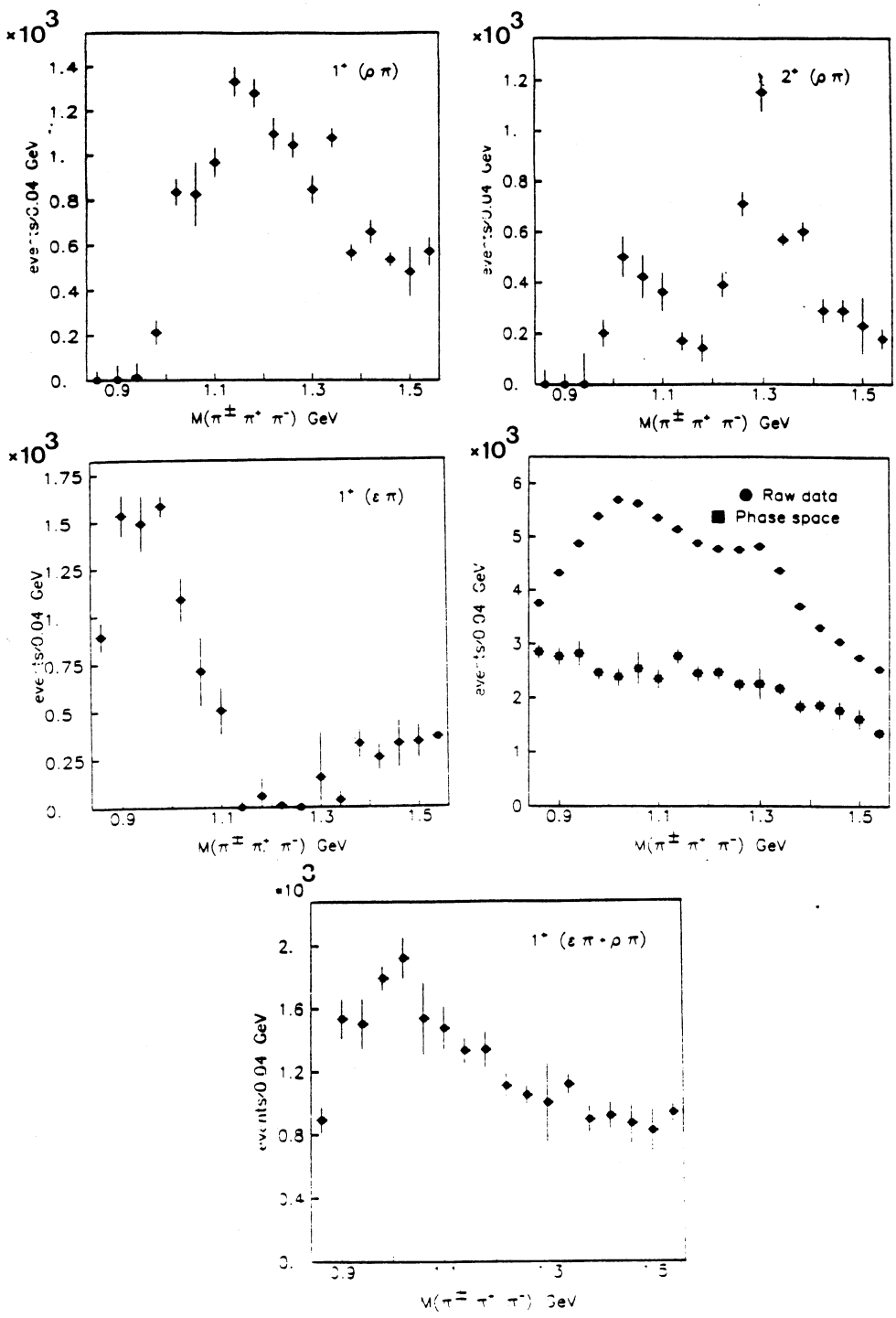

Figure 15: Results from the Dalitz plot analysis of the 3π system out of 4π centrally produced in WA76.

8. Physics with neutrals

In the 85 GeV/c run no γ detector was available to the WA76 experiment so that it was possible to reconstruct π^0's only as missing particles. The π^0 was reconstructed by assigning to it the missing momentum and the π^0 mass. The experimental resolution in the effective mass which makes use of such a π^0 has been estimated to be in the range 30 − 40 MeV so that the quality of these data is not so high as in the channels with only charged tracks.

The $\pi^+\pi^-\pi^0$ effective mass for the events with two central charged tracks after having removed the momentum balance events is shown in fig. 16a. The η and ω signals can be clearly seen and this plot shows that the experimental resolution is good enough to detect narrow structures, at least in the low mass region. The $K^+K^-\pi^0$ effective mass after having required that two particles be identified by the Cherenkov system as K or ambiguous K/p is shown in fig. 16b. A clear E signal can be seen with a possible hint of a D signal.

The $\eta\pi^+\pi^-$ system has been studied in the channel with 4 charged central pions and a reconstructed π^0. After having plotted all the $\pi^+\pi^-\pi^0$ combinations, the η region was selected and to the three particles in this region the η mass was assigned. The resulting $\eta\pi^+\pi^-$ effective mass summed over the two incident beams in shown in fig. 16c and shows clear $\eta'(958)$ and $f_1(1285)$ signals in spite of the large combinatorial background.

Since the physics in this channel is particularly interesting due to the problematics related to the existence of two pseudoscalar states observed to decay to $\eta\pi^+\pi^-$, a Dalitz plot analysis has been performed as a function of the $\eta\pi\pi$ mass. The results are summarized in fig. 16d on the 1^{++} and 0^{-+} projections and can be summarized as follows:

The 1^{++} wave shows a large structure at the $f_1(1285)$ mass with a possible hint of the presence od a 1^{++} $f_1(1420)$ signal. No evidence, on the other hand, is observed for pseudoscalar states. It is difficult, with these data to understand the effect of the experimental resolution on the results of the Dalitz plot analysis. Better data with a γ detector are needed in order to establish or not the existence of pseudoscalar states in this channel.

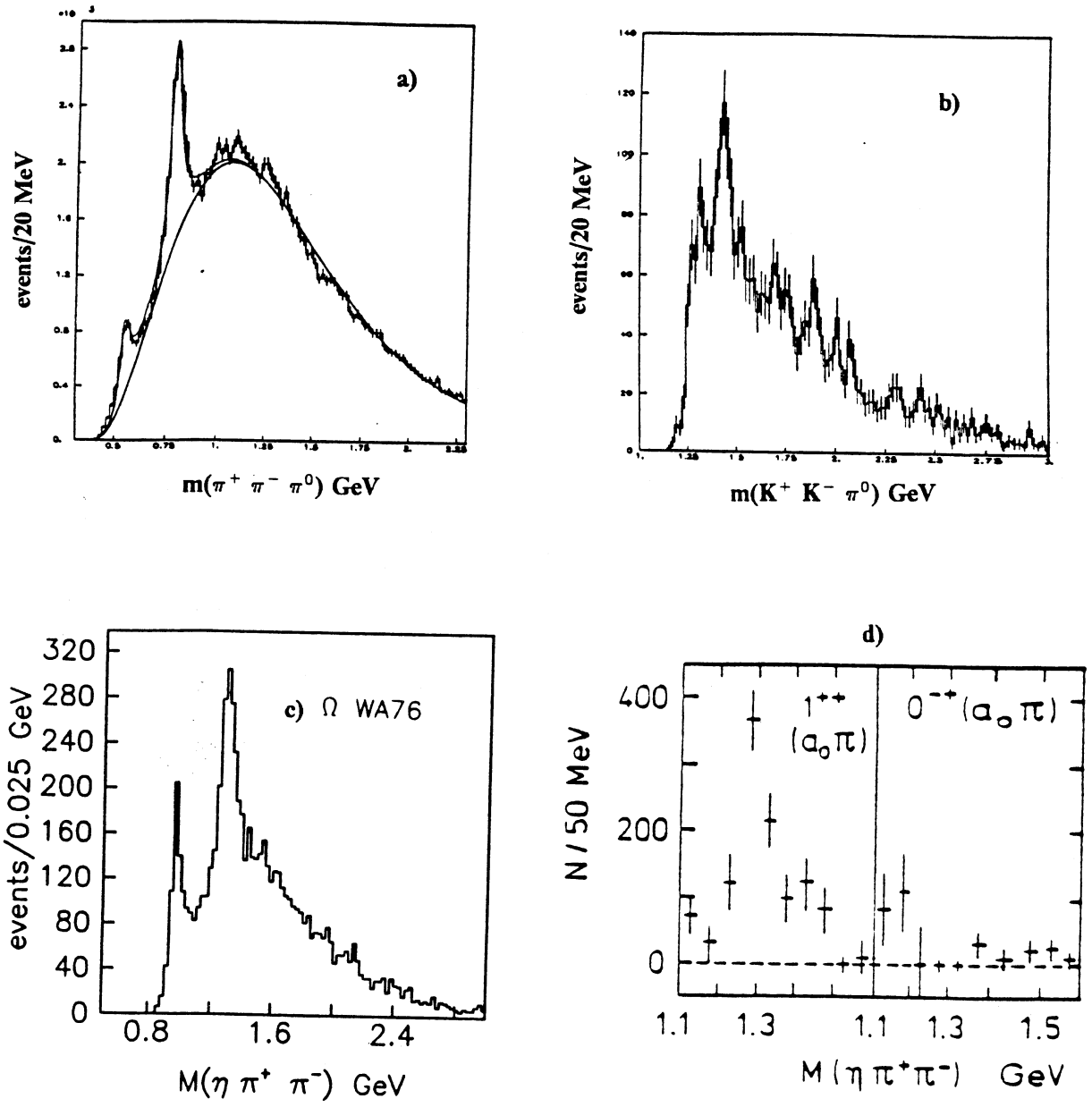

Figure 16: Physics with missing π^0's in WA76 at 85 GeV/c. a) $\pi^+\pi^-\pi^0$ effective mass, b) $K^+K^-\pi^0$ effective mass, c) $\eta\pi^+\pi^-$ effective mass, d) results from the Dalitz plot analysis of the $\eta\pi^+\pi^-$ system on the $J^{PC} = 1^{++}$ and 0^{-+} $a_0\pi$ projections.

9. Conclusions

A first look at the physics of the central region has been given by a run in Ω at 85 GeV/c. The results are encouraging, several states, including those on which discussions are actually going on in order to try to establish their quark – gluon composition, are clearly observed in particularly good conditions of signal to background. Further studies are needed in order to understand the dynamics which is at work to produce these states in the central region. A second run at 300 GeV/c has been performed to study the energy variation of the observed states and to search for new particles. In particular the resonances whose decays involve γ's should be detected.

10. References

[1] D. Robson et al., Nucl. Phys. B130 (1977) 328.

[2] D. Denegri et al., Nucl. Phys. B98 (1975) 189.

[3] D.M. Chew and G.F. Chew, Phys. Lett. 53B (1974) 191.

[4] T.A. Armstrong et al., Phys. Lett. 167B (1986) 133.

[5] W. Blum et al., Phys. Lett. 57B (1975) 403.

[6] M. Baubillier et al., Z. Phys. C17 (1983) 309.

[7] T.A. Armstrong et al., Phys. Lett. 66B (1986) 245.

[8] T.A. Armstrong et al., Z. Phys. C34 (1987) 33.

[9] A. Etkin et al., Phys. Rev. Lett. 40 (1978) 422;
A. Etkin et al., Phys. Rev. Lett. 41 (1978) 784.

[10] S.J. Lindenbaum, Comments Nucl. Part. Phys. 13 (1984) 285.

[11] T.H. Hansson et al., Phys. Rev. D26 (1982) 2069.

[12] T. Akesson et al., Nucl. Phys. B264 (1986) 154.

[13] K.L. Au et al., Phys. Rev. D35 (1987) 1633.

[14] S.M. Flatte' et al., Phys. Lett. 63 (1976) 224.

[15] U. Mallik, preprint SLAC – PUB – 4238 (1987).

[16] A. Palano, CERN − EP/87 − 92, 18 May 1987.

[17] D.L. Scharre et al., Phys. Lett. 97B (1980) 329;

C. Edwards et al., Phys. Rev. Lett. 49 (1982) 259.

[18] R. Armenteros et al., Int. Conf. on Elementary Particle Physics, Siena, Italy (1963);

P. Baillon et al., Nuovo Cim. 50A (1967) 393.

[19] S.U. Chung et al., Phys. Rev. Lett. 55 (1985) 779.

[20] A. Ando et al., Phys. Rev. Lett. 57 (1986) 1296.

[21] C. Dionisi et al., Nucl. Phys. B169 (1980) 1.

[22] D. Antreasyan et al., SLAC − PUB − 4305, May 1987.

[23] T.A. Armstrong et al., Phys. Lett. 146B (1984) 273.

T.A. Armstrong et al., Z. Phys. C34 (1987) 23.

[24] H. Aihara et al., Phys. Rev. Lett. 57 (1986) 51.

H. Aihara et al., Phys. Rev. Lett. 57 (1986) 2500.

G. Gidal et al., SLAC − PUB − 4275, April 1987.

[25] J.J. Becker et al., Phys. Rev. Lett. 59 (1987) 186.

[26] Ph. Gavillet at al., Z. Phys. C16 (1982) 119.

[27] D. Aston et al., SLAC − PUB − 4340, June 1987.

[28] C. Daum et al., Nucl. Phys. B182 (1981) 269.

[29] J. Dankowich et al., Phys. Rev. Lett. 46 (1981) 580.

[30] Ph. Gavillet et al., Phys. Lett. 69B (1977) 119.

[31] W. Ruckstuhl et al., Phys. Rev. Lett. 56 (1986) 2132.

[32] W.B. Schmidke et al., Phys. Rev. Lett. 57 (1986) 527.

[33] H. Albreckt et al., DESY 86 − 060 (1986) 527.